Supporting Information

Tailoring Chelating Sites in Two-Dimensional Covalent Organic Framework Nanosheets for Enhanced Uranium Capture

Ying Huang,[‡a] Jun Liao,[‡a] Jiahao Li,[‡b] Changming Cheng,[c] Yong Zhang*[a] and Yongwu Peng*[b]

[a]State Key Laboratory of Environment-friendly Energy Materials, School of National Defence Science & Technology, Southwest University of Science and Technology, Mianyang, 621010, PR China

[b]College of Materials Science and Engineering, Zhejiang University of Technology, Hangzhou 310014, PR China

[c]Institute of Nuclear Physics and Chemistry, China Academy of Engineering Physics (CAEP), Mianyang 612900, PR China

[‡]Ying Huang, Jun Liao, and Jiahao Li contributed equally to this work.

*Corresponding authors. E-mail: ywpeng@zjut.edu.cn; pandmzy@foxmail.com

Table of Contents

1. Experimental section

Chemicals

Tris(4-aminophenyl)amine (TAPA, 98%), 2,5-dihydroxyterethaldehyde (2,5-Dha, 98%), 1,2-dichlorobenzene (*o*-DCB, 99%), benzyl alcohol (99%), anisole (99%), 1-butanol (99%) and acetic acid (AA, 99.5%) were purchased from Tokyo Chemical Industry Co., Ltd. 2,3-Dihydroxyterethaldehyde (2,3-Dha, 98%) was purchased from Jilin Province Yanshen Technology Co, Ltd. $UO_2(NO_3)_2 \cdot 6H_2O$ (>99%) and arsenazo(III) (99.9%) were obtained from Hubei Chu Sheng Wei Chemistry Co., Ltd. All other chemicals were used as received without further purification.

Synthesis of 2D COF nanosheets

TAPA-COF-1 was synthesized by using a solvothermal method. A 10 mL Pyrex tube was charged with TAPA (6 mg, 0.02 mmol), 2,3-Dha (5 mg, 0.03 mmol) and o-dichlorobenzene/benzyl alcohol (4:1 v/v, 1 mL). The mixture was sonicated for 5 min to be dispersed homogeneously. Next, 0.1 mL of acetic acid (6 M) was added. Subsequently, the tube was flash-frozen at 77 K using a liquid N_2 bath and degassed by three freeze-pump-thaw cycles, sealed under vacuum, and then heated at 120 °C for 3 days. The precipitate was collected by centrifugation and washed with tetrahydrofuran. The collected sample was solvent-exchanged with acetone for 2-3 times and dried at 120 °C under vacuum for 12 h, and finally red powder was obtained (8.8 mg, 80% isolated yield).

TAPA-COF-2 was synthesized by using a solvothermal method. A 10 mL Pyrex tube was charged with TAPA (6 mg, 0.02 mmol), 2,5-Dha (5 mg, 0.03 mmol) and anisole/1-butanol (9:1 v/v, 1 mL). The mixture was sonicated for 5 min to be dispersed homogeneously. Next, 0.1 mL of acetic acid (6 M) was added. Subsequently, the tube was flash-frozen at 77 K using a liquid N_2 bath and degassed by three freeze-pump-thaw cycles, sealed under vacuum, and then heated at 120 °C for 3 days. The precipitate

was collected by centrifugation and washed with tetrahydrofuran. The collected sample was solvent-exchanged with acetone for 2-3 times and dried at 120 °C under vacuum for 12 h, and finally red powder was obtained (9.35 mg, 85% isolated yield).

Characterization methods

The powder X-ray diffraction (PXRD) patterns of TAPA-COF-1 and TAPA-COF-2 were recorded on a PANalytical XRD (Germany) equipped with a Cu Kα radiation (λ = 1.5406 Å) at a scan rate of 0.02^{o} s^{-1}. SEM images were obtained using a field emission scanning electron microscope (JSM-7600F). TEM images were observed on a transmission electron microscope (JEOL JEM-2100F). The Brunauer-Emmett-Teller (BET) surface areas of TAPA-COF-1 and TAPA-COF-2 were calculated from N_2 sorption isotherms at 77 K using a Micromeritics ASAP 2020 surface area. Fourier transform infrared spectroscopy (FTIR) spectra were collected on an FT-IR spectrometer (PerkinElmer Spectrum GX) in the range of 400-4000 cm^{-1}. Thermogravimetric analyses (TGA) were recorded by a TA instrument (TGA 2950) with a heating rate of 10 °C min^{-1}.

Structure determination

The structure of TAPA-COF-1 and TAPA-COF-2 was measured using the Materials Studio Visualizer. The TAPA-COF-1 and TAPA-COF-2 were modeled with a P3/P6 unit cell conceived from the native connectivity and geometry of the building blocks. The structure was geometrically optimized using the MS Forcite molecular dynamics module (Universal force fields, Ewald summations). The obtained unit cell parameters and selected atom sites of TAPA-COF-1 and TAPA-COF-2 are summarized in Table S1 and Table S2.

Adsorption experiments

In order to evaluate the adsorption performance of TAPA-COF-1 and TAPA-COF-2 for U(VI) capture, the batch adsorption experiments were performed in U(VI) solution

under ambient conditions. The influence factors including initial pH, adsorbent dosage, competitive ions, ionic strength, initial concentration of U(VI) and contact time on U(VI) were investigated. The pH of the initial U(VI) solution was adjusted by adding HCl or NaOH and measured by a pH meter. The batch adsorption experiments were carried out by adding a certain amount of adsorbents (TAPA-COF-1 or TAPA-COF-2) into 100 mL of U(VI) solution. After adsorption, the equilibrium concentration of U(VI) in the supernatants was determined by using UV-vis spectrophotometer at 651 nm with arsenazo(III) (0.1 %) as the chromogenic agent. It was worth mentioning that all of the adsorption experiments were carried out in triplicate and the results were obtained by the average of triplicate determination. The adsorption capacity (q_e, mg g^{-1}) and adsorption efficiency (AE, %) were calculated using the following equations:

$$q_e = \frac{C_0 V - C_e V}{m} \quad (1)$$

$$AE = \frac{(C_0 - C_e)}{C_0} \times 100\% \quad (2)$$

Where C_0 and C_e is the initial and equilibrium concentrations of U(VI) species, respectively, V is the volume of U(VI) and m is the mass of the adsorbents.

Theoretical calculation

The density functional theory (DFT) calculations were carried out using a Dmol3 module of Material Studio. The adsorption energy (E_{ads}) was calculated by the following formula:

$$E_{ads} = E_{complex} - (E_{substrate} + E_{adsorbate}) \quad (3)$$

Where $E_{substrate}$, $E_{adsorbate}$ and $E_{complex}$ stand for the total electronic energy of TAPA-COF-1 or TAPA-COF-2, U(VI) and their complex, respectively.

2. Characterization of 2D COF nanosheets

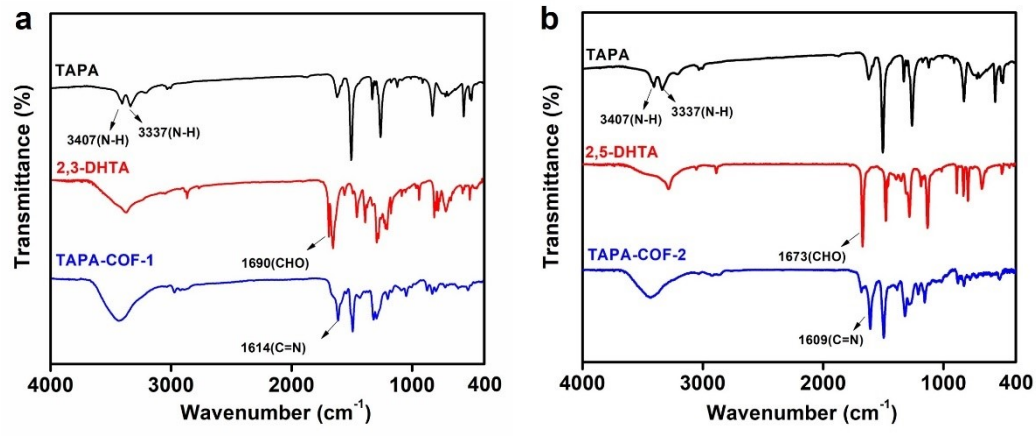

Figure S1. FT-IR spectra of the as-prepared TAPA-COF-1 (a), TAPA-COF-2 (b) and molecular building units (a and b).

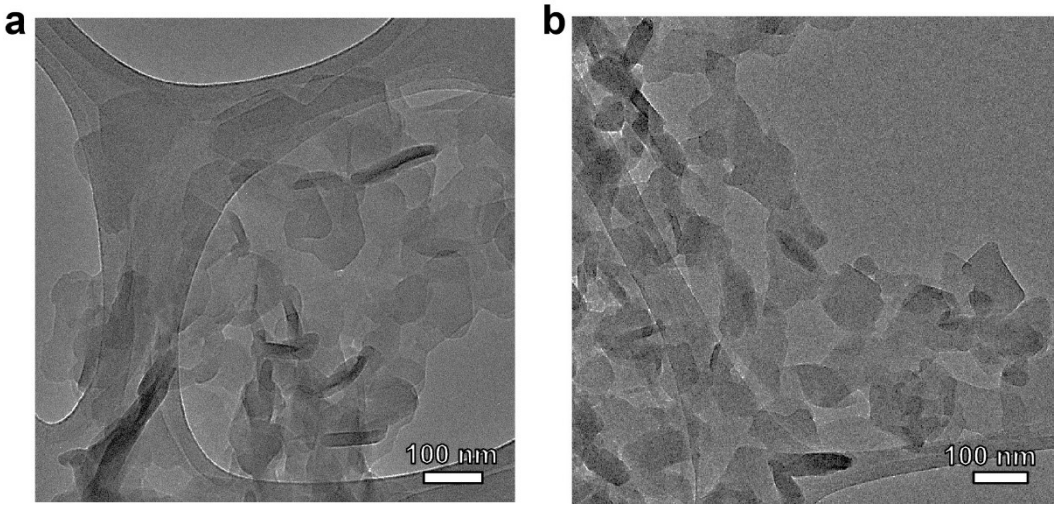

Figure S2. TEM images of TAPA-COF-1 (a) and TAPA-COF-2 (b).

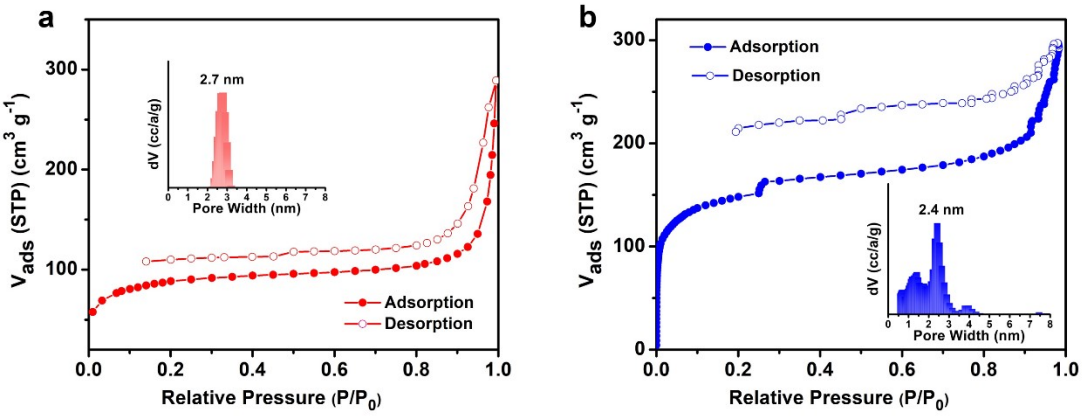

Figure S3. N_2 sorption isotherms of TAPA-COF-1 (a) and TAPA-COF-2 (b). Inset: Pore size distribution profiles of TAPA-COF-1 (a) and TAPA-COF-2 (b).

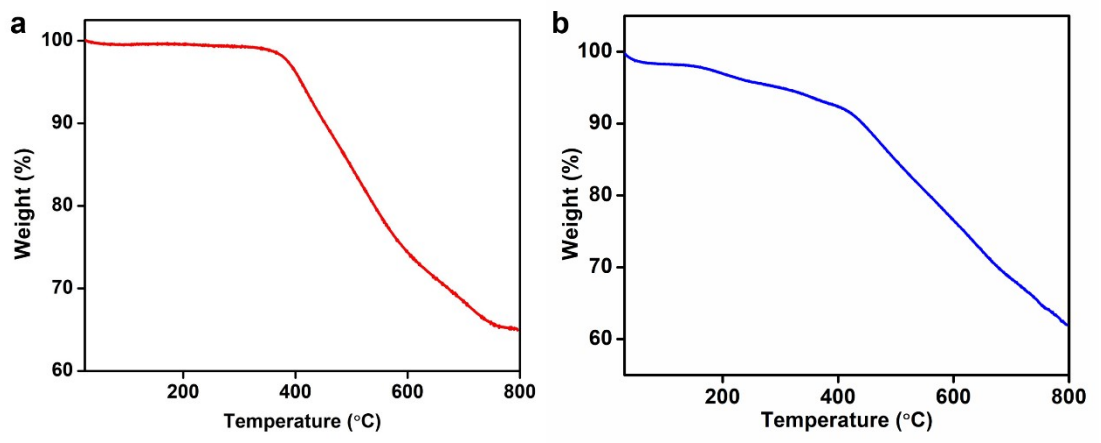

Figure S4. TGA analysis of TAPA-COF-1 (a) and TAPA-COF-2 (b).

Table S1. Atom sites for the modeled TAPA-COF-1 nanosheets.

Space group		*P*3	
Calculated unit cell		$a = b = 32.3417$ Å; $c = 3.9636$ Å $\alpha = \beta = 90°$; $\gamma = 120°$	
Atoms	X	Y	Z
C	0.63658	0.28139	0.37246
C	0.65107	0.25216	0.52976

C	0.62234	0.20252	0.52914
C	0.57815	0.18045	0.37291
C	0.56325	0.20912	0.21301
C	0.59213	0.25879	0.2139
N	0.44533	0.57441	0.30258
C	0.49161	0.59548	0.31015
C	0.51645	0.56758	0.31251
C	0.49582	0.52147	0.44917
C	0.52196	0.49686	0.45158
C	0.35648	0.71874	0.30181
C	0.33553	0.74235	0.45917
C	0.35742	0.79209	0.45818
C	0.40133	0.81974	0.30128
C	0.42305	0.79689	0.15055
C	0.40069	0.74711	0.14703
N	0.57882	0.44965	0.38043
C	0.59539	0.49295	0.27524
C	0.56689	0.51726	0.29558
C	0.58627	0.56284	0.15887
C	0.56179	0.58799	0.17252
O	0.94842	1.49484	0.61668
O	1.05139	1.55022	0.57937
H	0.68711	0.2687	0.66287
H	0.63518	0.1795	0.65872
H	0.52719	0.1921	0.07984
H	0.57853	0.28091	0.08054
H	0.51374	0.63612	0.3151
H	0.2997	0.72098	0.59267
H	0.33928	0.81036	0.58675
H	0.4596	0.81873	0.02739
H	0.41936	0.72972	0.0138
H	0.63283	0.51345	0.16329
H	0.62283	0.58022	0.0328

H	0.57944	0.62582	0.06688
H	0.97275	1.52743	0.76195
H	1.02678	1.55909	0.71481
N	0.66667	0.33333	0.3727
N	0.33333	0.66667	0.30125

Table S2. Atom sites for the modeled TAPA-COF-2 nanosheets.

Space group		*P*6	
Calculated unit cell		$a = b = 32.7057$ Å; $c = 3.8393$ Å $\alpha = \beta = 90°$; $\gamma = 120°$	
Atoms	X	Y	Z
C	0.63658	0.28139	0.37246
C	0.65107	0.25216	0.52976
C	0.62234	0.20252	0.52914
C	0.57815	0.18045	0.37291
C	0.56325	0.20912	0.21301
C	0.59213	0.25879	0.2139
N	0.44533	0.57441	0.30258
C	0.49161	0.59548	0.31015
C	0.51645	0.56758	0.31251
C	0.49582	0.52147	0.44917
C	0.52196	0.49686	0.45158
C	0.35648	0.71874	0.30181
C	0.33553	0.74235	0.45917
C	0.35742	0.79209	0.45818
C	0.40133	0.81974	0.30128
C	0.42305	0.79689	0.15055
C	0.40069	0.74711	0.14703
N	0.57882	0.44965	0.38043
C	0.59539	0.49295	0.27524
C	0.56689	0.51726	0.29558

C	0.58627	0.56284	0.15887
C	0.56179	0.58799	0.17252
O	0.94842	1.49484	0.61668
O	1.05139	1.55022	0.57937
H	0.68711	0.2687	0.66287
H	0.63518	0.1795	0.65872
H	0.52719	0.1921	0.07984
H	0.57853	0.28091	0.08054
H	0.51374	0.63612	0.3151
H	0.2997	0.72098	0.59267
H	0.33928	0.81036	0.58675
H	0.4596	0.81873	0.02739
H	0.41936	0.72972	0.0138
H	0.63283	0.51345	0.16329
H	0.62283	0.58022	0.0328
H	0.57944	0.62582	0.06688
H	0.97275	1.52743	0.76195
H	1.02678	1.55909	0.71481
N	0.66667	0.33333	0.3727
N	0.33333	0.66667	0.30125

3. Adsorption performance

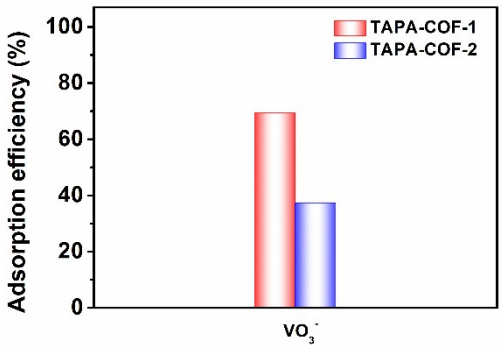

Figure S5. Effect of VO_3^- on the adsorption of U(VI) by using TAPA-COF-1 and TAPA-COF-2 (C_0 = 10 mg/L, m/V = 0.1 g/L and pH = 6).

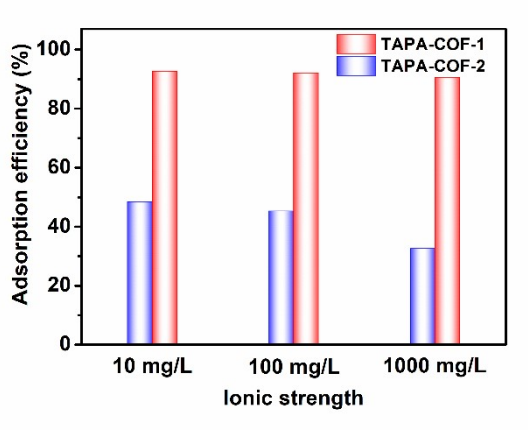

Figure S6. Effect of ionic strength on the adsorption of U(VI) by using TAPA-COF-1 and TAPA-COF-2 (C_0 = 10 mg/L, m/V = 0.1 g/L and pH = 6).

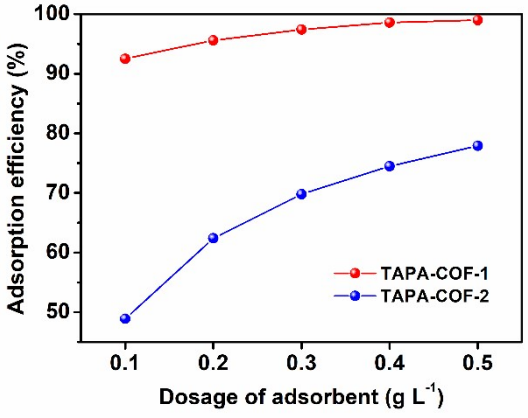

Figure S7. Effect of adsorbent dosage on the adsorption of U(VI) (C_0 = 10 mg/L and pH = 6).

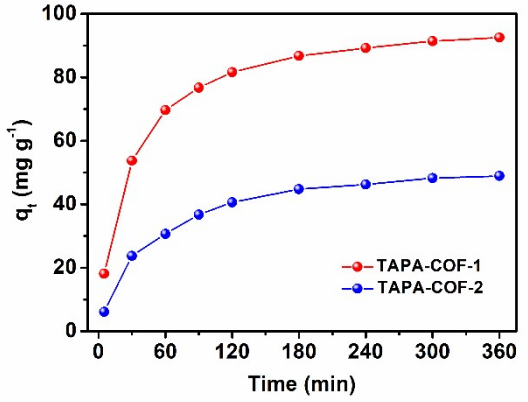

Figure S8. Effect of contact time on the adsorption of U(VI) by using TAPA-COF-1 and TAPA-COF-2 (C_0 = 10 mg/L, m/V = 0.1 g/L and pH = 6)

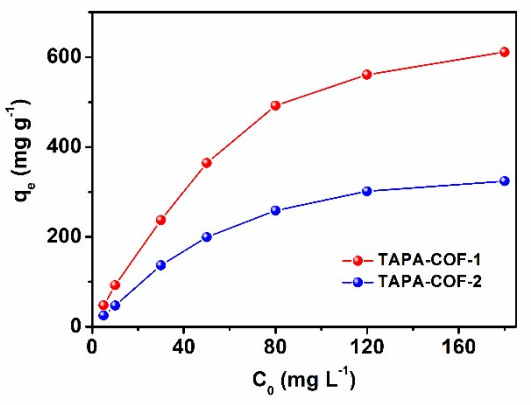

Figure S9. Effect of initial U(VI) concentration on the adsorption of U(VI) by using TAPA-COF-1 and TAPA-COF-2 (m/V = 0.1 g/L and pH = 6).

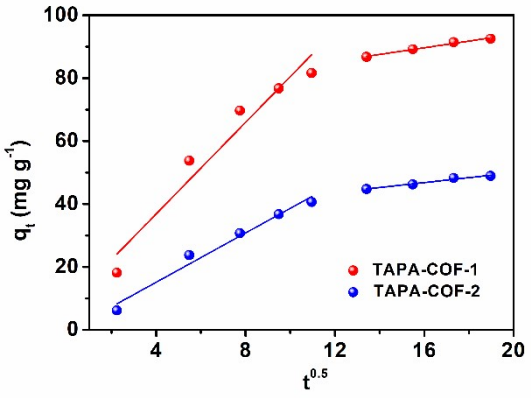

Figure S10. Intraparticle diffusion kinetic model (C_0 = 10 mg/L, m/V = 0.1 g/L and pH = 6).

Table S3. Kinetic parameters of U(VI) adsorption on TAPA-COF-1 and TAPA-COF-2.

Samples	PSO model			PFO model		
	K_2 (g min^{-1} mg^{-1})	q_e (mg g^{-1})	R^2	q_e (mg g^{-1})	K_1 (min^{-1})	R^2
TAPA-COF-1	0.000414	98.5	0.999	88.5	0.028	0.970
TAPA-COF-2	0.00043	54.7	0.997	47.3	0.019	0.980

Table S4. Isotherm parameters of U(VI) adsorption on TAPA-COF-1 and TAPA-COF-2.

Models	samples	Parameters			
		q_m (mg g^{-1})	K_L (L g^{-1})	-	R^2
Langmuir	TAPA-COF-1	657.2	0.096	-	0.997
	TAPA-COF-2	400.7	0.032	-	0.986
			K_F (mg^{1-n} L^n g^{-1})	n_F	R^2
Freundlich	TAPA-COF-1	-	143.7	3.13	0.953
	TAPA-COF-2	-	38.6	2.25	0.930

Table S5. Comparison of different COF-based absorbents for U(VI) adsorption.

Adsorbents	Adsorption capacity (mg g^{-1})	Ref.
COF-TpDb-AO	408	1
COF-PDAN-AO	410	2
TP-COF-AO	436	3
Dp-COF	317.3	4
TpDAB	461.4	5
TpPy	291.79	6
CNT/COF-OH	518.2	7
TPB-BPTA-COF-AO	319.9	8

COF-DBD-AO	250.7	9
HDU-102-AO	389.08	10
MhBd	314	11
JUC-505-COOH	464	12
2,3-DhaTat-COF	640	13
TAPA-COF-1	657.2	This work

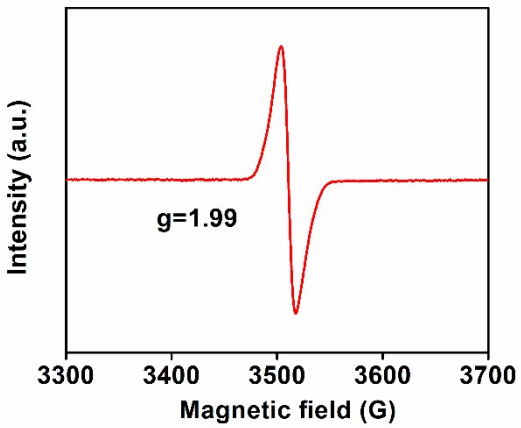

Figure S11. EPR spectrum of TAPA-COF-1 after uranium adsorption.

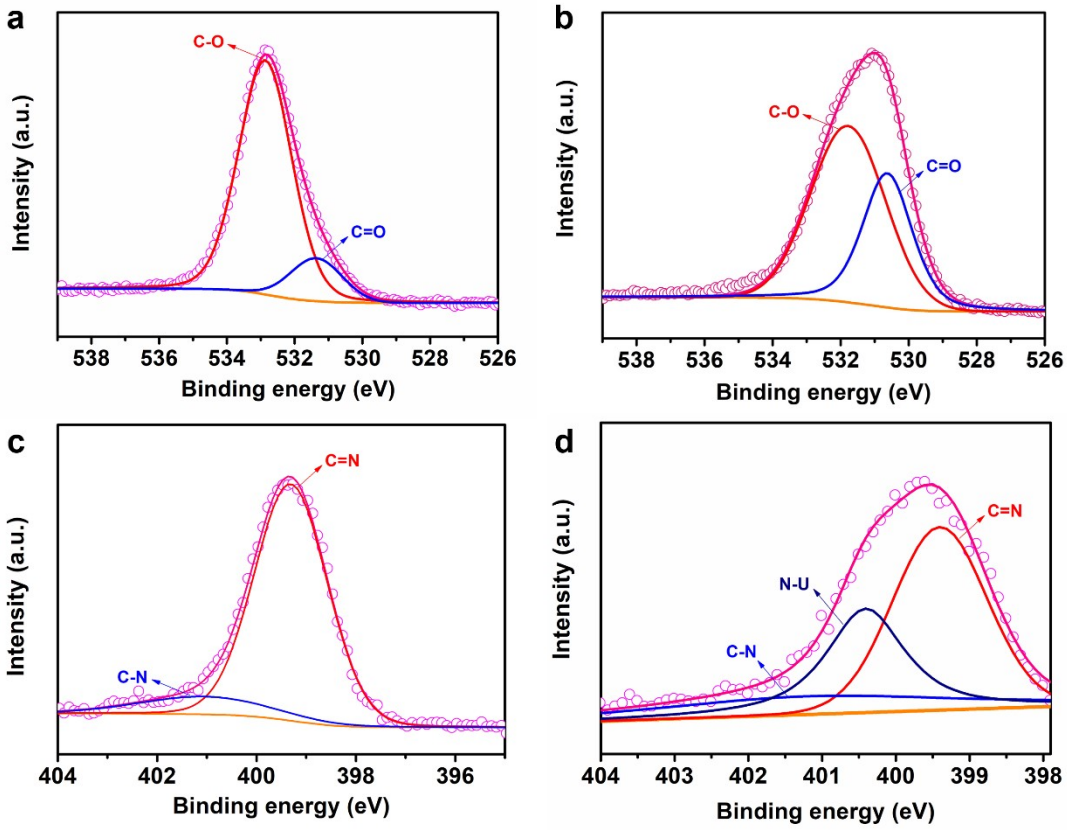

Figure S12. (a and b) High-resolution O 1s XPS spectra of TAPA-COF-1 before (a) and after (b) U(VI) adsorption. (c and d) High-resolution N 1s XPS spectra of TAPA-COF-1 before (c) and after (d) U(VI) adsorption.

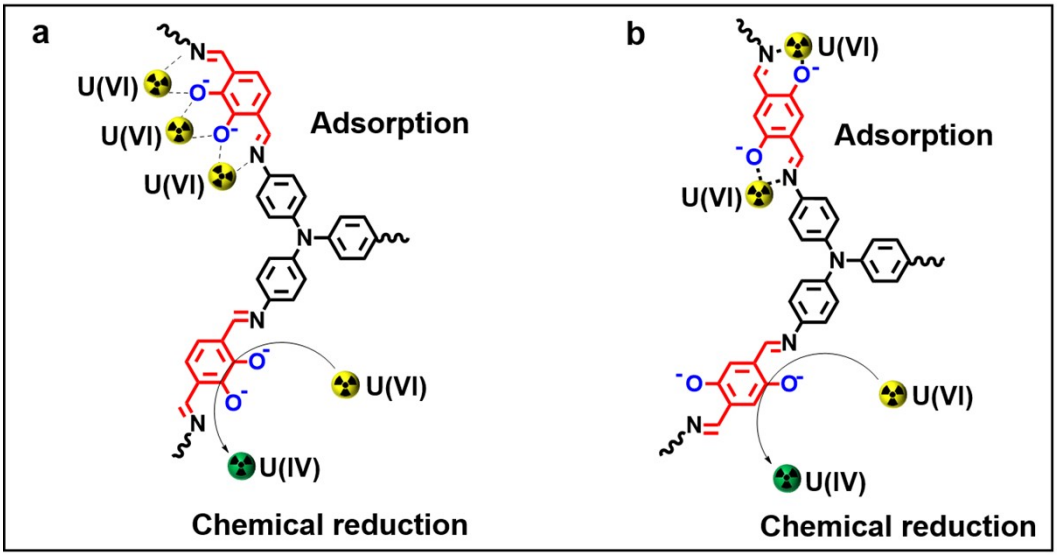

Figure S13. Schematic diagram of uranium capture mechanism by (a) TAPA-COF-1 and (b) TAPA-COF-2.

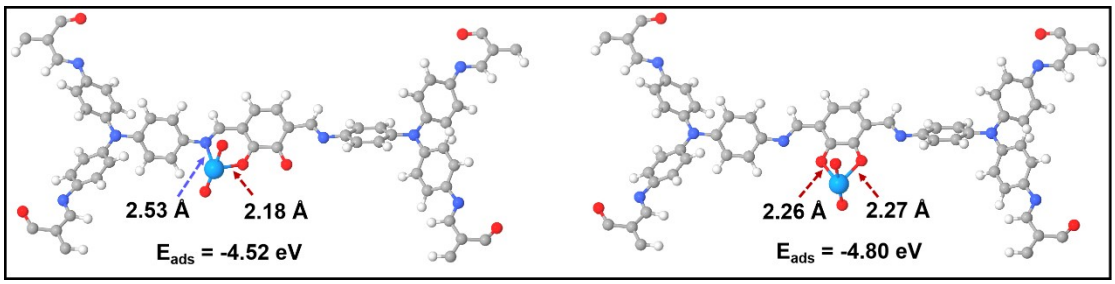

Figure S14. Adsorption energy between U(VI) and TAPA-COF-1 calculated by DFT method.

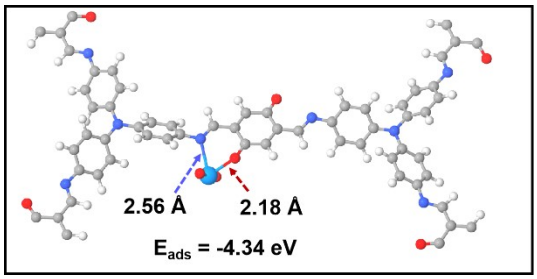

Figure S15. Adsorption energy between U(VI) and TAPA-COF-2 calculated by DFT method.

4. References

1. Q. Sun, B. Aguila, L. D. Earl, C. W. Abney, L. Wojtas, P. K. Thallapally and S. Ma, *Adv. Mater.*, 2018, **30**, 1705479.
2. F.-F. Li, W.-R. Cui, W. Jiang, C.-R. Zhang, R.-P. Liang and J.-D. Qiu, *J. Hazard. Mater.*, 2020, **392**, 122333.
3. C.-R. Zhang, W.-R. Cui, W. Jiang, F.-F. Li, Y.-D. Wu, R.-P. Liang and J.-D. Qiu, *Environ. Sci. Nano*, 2020, **7**, 842-850.
4. J. Zhang, L. Zhou, Z. Jia, X. Li, Y. Qi, C. Yang, X. Guo, S. Chen, H. Long and L. Ma, *Nanoscale*, 2020, **12**, 24044-24053.
5. R.-H. Yan, W.-R. Cui, C.-R. Zhang, X.-J. Li, J. Huang, W. Jiang, R.-P. Liang and J.-D. Qiu, *Chem. Eng. J.*, 2021, **420,** 129658.

6. R. Guo, Y. Liu, Y. Huo, A. Zhang, J. Hong and Y. Ai, *J. Colloid Interface Sci.*, 2022, **606**, 1617-1626.
7. X. Liu, X. Wang, W. Jiang, C.-R. Zhang, L. Zhang, R.-P. Liang and J.-D. Qiu, *Chem. Eng. J.*, 2022, **450**, 138062.
8. X. Qin, X. Tang, Y. Ma, H. Xu, Q. Xu, W. Yang and C. Gu, *Chem. Res. Chin. Univ.*, 2022, **38**, 433-439.
9. S. Y. Wang, G. Wei, Y. H. Xie, H. L. Shang, Z. S. Chen, H. Q. Wang, H. Yang, G. I. N. Waterhouse and X. K. Wang, *Sep. Purif. Technol.*, 2022, **303**, 122256.
10. C. Wang, W. Xi, R. Guo, S. Wang, W. Lu, Y. Bai and J. Wang, *J. Radioanal. Nucl. Chem.*, 2022, **331**, 2469-2478.
11. L. Zhang, S.-L. Wang, G.-H. Zhang, N. Shen, H. Chen, G. Tao, G.-H. Tao, F. Yong, J. Fu, Q.-H. Zhu and L. He, *Cell Rep. Phys. Sci.*, 2022, **3**. 101114.
12. Z. Y. Li, R. M. Zhu, P. L. Zhang, M. Yang, R. Q. Zhao, Y. L. Wang, X. Dai and W. Liu, *Chem. Eng. J.*, 2022, **434**, 134623.
13. X. Lin, W. Xin, S. Chen, Y. Song, L. Yang, Y. Qian, L. Fu, Y. Cui, X. He, T. Li, Z. Zhang, Y. Wu, X.-Y. Kong, L. Jiang and L. Wen, *J. Hazard. Mater.*, 2023, **458**, 131978.